


Faithfully Simulating Near-Term Quantum Repeaters

Julius Wallnöfer^{1,*}, Frederik Hahn^{1,2}, Fabian Wiesner^{1,2}, Nathan Walk,¹ and Jens Eisert^{1,3}

¹*Dahlem Center for Complex Quantum Systems, Freie Universität Berlin, Arnimallee 14, 14195 Berlin, Germany*

²*Electrical Engineering and Computer Science Department, Technische Universität Berlin, 10587 Berlin, Germany*

³*Helmholtz-Zentrum Berlin für Materialien und Energie, Hahn-Meitner-Platz 1, 14109 Berlin, Germany*

 (Received 6 March 2023; revised 8 November 2023; accepted 23 January 2024; published 27 March 2024)

Quantum repeaters have long been established to be essential for distributing entanglement over long distances. Consequently, their experimental realization constitutes a core challenge of quantum communication. However, there are numerous open questions about implementation details for realistic near-term experimental setups. In order to assess the performance of realistic repeater protocols, here we present *ReQuSim*, a comprehensive Monte Carlo–based simulation platform for quantum repeaters that faithfully includes loss and models a wide range of imperfections such as memories with time-dependent noise. Our platform allows us to perform an analysis for quantum repeater setups and strategies that go far beyond known analytical results: This refers to being able to both capture more realistic noise models and analyze more complex repeater strategies. We present a number of findings centered around the combination of strategies for improving performance, such as entanglement purification and the use of multiple repeater stations, and demonstrate that there exist complex relationships between them. We stress that numerical tools such as ours are essential to model complex quantum communication protocols aimed at contributing to the quantum Internet.

DOI: [10.1103/PRXQuantum.5.010351](https://doi.org/10.1103/PRXQuantum.5.010351)

I. INTRODUCTION

Quantum communication constitutes one of the core subfields of the quantum technologies. A cornerstone of virtually every large-scale quantum research effort around the world, its most compelling applications include secure communication via quantum key distribution [1–3] as well as other multiparty cryptographic primitives [4,5] and even functionality for secure distributed quantum computing [6]. Indeed, distributed and entangled quantum systems allow us to establish secure encryption keys based on fundamental physical principles. With respect to real-world implementations of key distribution over arbitrary distances—in particular, arbitrary locations on earth—it was realized early on that techniques would be needed that can combat unavoidable losses and errors. In the quantum setting, classical strategies of signal amplification as used in classical repeaters are not applicable and so the idea of a *quantum repeater* has been devised [7–10].

While already, to date, impressive implementations of direct quantum communication have been achieved [11–13], there are limits to this approach. It is only with the help of such quantum repeaters that fundamental limits being governed by the *repeaterless bound*, the so-called PLOB bound [14] (see Refs. [15,16] for a strong converse), can be overcome. Indeed, it is seen that the ultimate limits in the presence of repeaters are substantially more favorable [17,18]. Since the first repeater proposals, substantial research effort has been dedicated to experimentally realizing full-scale quantum repeaters. These realizations remain a major technological challenge and, therefore, one of the main goals of the quantum communications field is to overcome this significant bottleneck [2,3,19]. These technological challenges are not so much conceptual—the basic principles have been known for a long time—but arise from the complicated interplay of the components, which include quantum light and, usually, matter qubits. This central bottleneck is, therefore, primarily one of quantum engineering in the field of quantum optics and light-matter interactions—albeit a persistent and difficult one.

From a high-level perspective, there are indeed a number of open challenges when considering more advanced repeater schemes. For one, there are many design features for variants of repeater protocols that can be modified or combined. Also, it is very difficult to compare advantages

*julius.wallnoefer@fu-berlin.de

Published by the American Physical Society under the terms of the [Creative Commons Attribution 4.0 International license](https://creativecommons.org/licenses/by/4.0/). Further distribution of this work must maintain attribution to the author(s) and the published article's title, journal citation, and DOI.

between vastly different platforms involving trapped ions, nitrogen-vacancy (NV) centers, silicon-based systems, or atomic gases. For simple paradigmatic problems, some settings can be analytically studied, even involving some experimentally relevant parameters [9,20–24]. Beyond such paradigmatic settings, an analytical study seems to be out of reach. In contrast, several large-scale initiatives that are aiming at realizing quantum networks within the quantum Internet—such as the *Quantum Internet Alliance* or the *Quantum Internet Task Force*—have set-up simulation schemes for simulating high-level quantum communication protocols. Naturally, they differ in scope and goals as well as the models and abstractions used. Other simulation tools, such as *NetSquid* [25], *QuISP* [26] and *SeQUeNCe* [27], have been used to great effect to study various aspects of quantum networks (for a more detailed discussion, see Sec. V).

With *ReQuSim*, we present an event-based Monte Carlo simulation platform for realistic quantum repeaters, which is versatile enough to study complex repeater schemes for realistic small-to-intermediate-scale quantum networks and that is, first and foremost, faithful to a wide range of physically relevant parameters on the hardware level of quantum repeaters. This platform allows us to compare different physical architectures fairly, to explore new regimes, and to identify new possibly unexpected schemes in the first place. In *ReQuSim*, we combine *scale* with *realism*. With respect to realism, the platform is detailed enough to, in particular, include arbitrary time-dependent decoherence mechanisms as opposed to a simple waiting-time loss model. This facilitates the modeling of heterogeneous networks incorporating multiple physical realizations for communication channels and network nodes. With regard to scale, our analysis in this work includes schemes of up to 32 repeater links; however, we demonstrate the runtime scaling of up to 1024 repeater links in Appendix B. Therefore, we consider our simulation scheme to be useful for any quantum network scenario expected to exist in the short to medium term.

Analyzing such near-term scenarios with realistic error models is precisely the focus of our method. While there are existing numerical analyses on the use of realistic devices for quantum repeaters (see, e.g., Refs. [25,27–29]), the sheer variety of potential approaches and the fact that their performance is strongly dependent on the precise circumstances make further investigation of these concepts indispensable.

We stress that we can do more than just simulating what will happen in a given scenario with certain resources. Instead, we are able to simulate a host of scenarios and give actionable advice on what *should* be done with a given set of equipment to maximize performance. This point is critical for establishing whether implementing new methods actually lead to improved results for actual applications. We demonstrate such a case in Sec. IV A, where we

consider a repeater scheme with a single repeater station that can optionally make use of entanglement purification as an additional tool. While this certainly increases the complexity of the scheme, there are clear circumstances in which it outperforms a naive scheme using only entanglement swapping. However, discarding qubits in memory after a certain cutoff time is an alternative method that can be used to reduce the error rates at the cost of throughput. A proper optimization over cutoff times (a relatively simple software adjustment instead of requiring new operations) can see the relative advantage shrink or vanish. In this case, the overall performance would not be meaningfully improved by the expenditure of additional resources on employing entanglement purification methods. This kind of detailed benchmarking is essential to properly evaluate under which circumstances a particular building block should be utilized.

With *ReQuSim*, we can provide guidance in a meaningful strategy analysis. The use of multiple repeater stations instead of one can extend the reachable distances but will also subject the process to additional noise from storing more qubits in memory and performing more operations. In Sec. IV B, we explore this trade-off and show that the number of repeater stations needs to be carefully optimized if their quality is limited, even if their quantity is not. Furthermore, we demonstrate that improving the quality of those repeater-station resources results in a disproportionate improvement in achievable rates, as it allows us to modify the protocol to use a larger number of repeater stations, which would otherwise be detrimental. In a similar vein, in Sec. IV C we demonstrate how our approach can be used to give insight about necessary hardware parameters in a setting with a customized noise model.

Considering the above points, it is clear that there is no shortage of potential options to improve performance. As the examples shown in this work compellingly demonstrate, there are highly nontrivial relationships between *combinations* of these strategies. Optimizing repeater protocols for a variety of realistic devices therefore requires a deeper understanding of repeater protocols and is not simply a matter of tweaking a few parameters.

II. ReQuSim: THE SIMULATION FRAMEWORK

ReQuSim [30] is a simulation framework that we have developed specifically for simulating quantum repeaters. It is available as an open-source PYTHON package from the Python Package Index. Simulating quantum repeaters is a very attractive option, as the complexity of analytical expressions is increasing rapidly if one deviates from the known standard cases. A central challenge in this regard is that everything that happens anywhere in the system can potentially effect parts on the opposite end of the repeater chain, e.g., the time a qubit needs to wait in memory.

Working with averages calculated for parts of the system does not necessarily give the full picture if there are nonlinearities such as the dephasing in quantum memories. By contrast, Monte Carlo methods are well suited to deal with systems with many interconnected probabilistic components. The simulation approach further allows for a modular design that makes switching to different error models and introducing asymmetries straightforward.

In the following, we describe the basic working principles of the simulation. First, the various parts needed for the given scenario are initialized, e.g., where the end stations and repeater stations are located. This also includes setting up the noise models that are specific to certain devices, such as the dephasing time for quantum memories.

The core of the simulation relies on an event system with which the repeater protocol can interact. Changes to the state of the simulation are done via events that represent operations being performed. These are scheduled in an event queue and later resolved at the appropriate time. Naturally, an event needs to have the information about when to resolve and which are the involved quantum states and repeater stations. For example, an entanglement swapping event would follow the data structure (type, time, pairs, station). What exactly occurs when an event resolves will depend on the type of the event, e.g., an entanglement purification event will simulate the required quantum operations and measurements for an entanglement purification protocol on the involved quantum states.

The other moving part of the system is the repeater protocol, i.e., the high-level strategy, the simulation should follow, because this defines which events should be scheduled and when. Naturally, the chosen repeater strategy decides which events exactly are used; e.g., a repeater

protocol without entanglement purification may decide to schedule an entanglement swapping event at a station, immediately after entangled pairs in both directions have been established. Alternatively, in Fig. 1, the high-level strategy of a repeater protocol following a layered approach for entanglement swapping is illustrated.

The way in which the simulation moves forward revolves around a constant interaction of the protocol and the event system. This means that after an event is resolved, the protocol immediately checks whether any new events need to be scheduled, i.e., the protocol will continuously monitor the changes performed by the last event. An abstract representation of how this core simulation loop and the decision-making process of a simple repeater protocol works is described in Fig. 2.

While protocols are usually formulated from a high-level point of view similar to the situation depicted in Fig. 1, due to the probabilistic nature at multiple parts of the simulation, e.g., the initial distribution process, the actual simulation process needs to be able to act and react at a more detailed level. Consider as an example the situation in Fig. 3. While multiple pairs between stations A and C_2 have been established, the protocol is currently waiting for progress on the right-hand side before it can proceed further. After a source event confirms the successful generation of an entangled pair between stations C_2 and C_3 , the protocol reacts by scheduling entanglement swapping events at stations C_2 and C_3 , since these are now finally possible. Since these can be performed immediately, they are inserted at the front of the event queue, pushing back the other events that happen at a later point in simulated time. Then, the entanglement swapping events are resolved one by one and after each one the protocol checks whether anything new needs to be done—in this case, no new

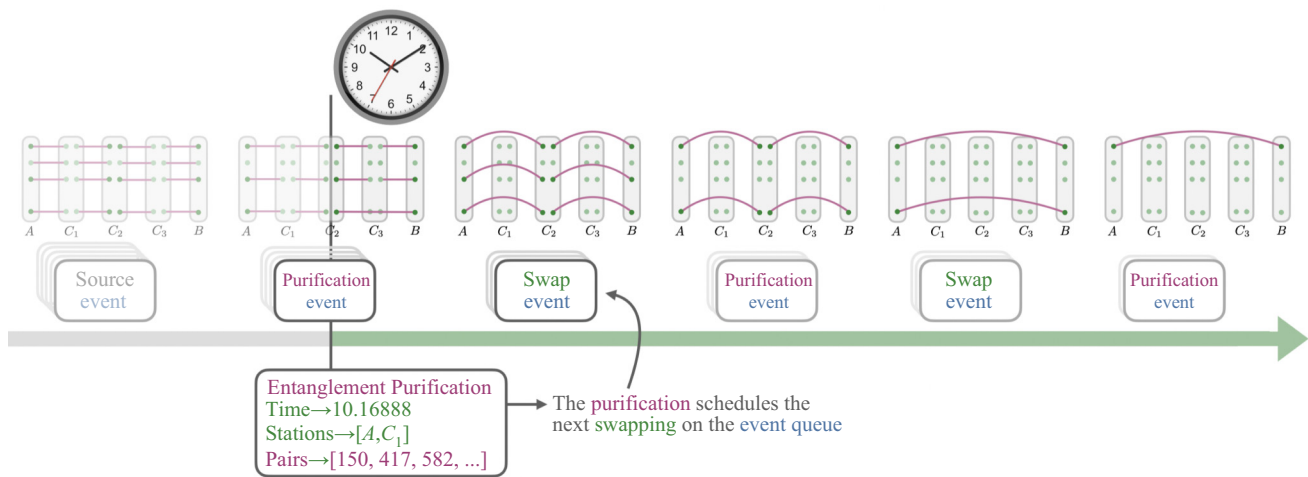


FIG. 1. An entanglement-swapping-based repeater protocol in the *ReQuSim* simulation framework. Running the protocol schedules first events on the event queue. The events on the queue are successively resolved and may schedule further events. An example of this is highlighted above for an entanglement purification event scheduling an entanglement swapping event.

Algorithm Run multimemory repeater

```

scenario ← Setup including, e.g., position of stations and sources
iter ← desired number of long-distance entangled connections
params ← parameters of the model as described in Sec. III
protocol ← description of the repeater protocol to perform
function RUN(scenario, iter, params, protocol)
  INITIALIZE setup according to scenario and params
  l ← number of successfully established links starting at 0
  while l < iter do
    protocol.CHECK for new events to be scheduled
    if long-distance connection has been established then
      UPDATE collected data.
      l ← l + 1
    RESOLVE next event in event queue
function CHECK (example for a single station)
  nmem ← number of quantum memories per link at station
  nl,r ← number of established pairs left and right of station
  sl,r ← number of events creating pairs left and right of station
  (i.e., accounting for busy memories with no established pair)
  if nl + sl < nmem then
    SCHEDULE source events drawing from time distribution
  if nr + sr < nmem then
    SCHEDULE source events drawing from time distribution
  if nl > 0 and nr > 0 then
    SCHEDULE entanglement-swapping event
  
```

FIG. 2. The pseudocode for formulating a protocol and running the simulation. This example describes a protocol for a single repeater station that has access to multiple quantum memories to simultaneously attempt to establish an entangled connection for both repeater links and immediately performs entanglement swapping once successful qubits for both directions are in memory. The *events* are standardized ways to interact with the current state of the simulation. They have a method that specifies the associated quantum operation that is performed on the quantum states when they are resolved, e.g., a Bell-state measurement for the entanglement swapping event.

events need to be scheduled. Finally, the event system goes back to resolving the previously scheduled events in the event queue.

The output of the simulation is a sample of the time and state distributions that is produced by the repeater setup. This means that one gets a list of states (if distributing entangled pairs) or error probabilities (if measuring qubits arriving at the end stations as soon as possible, as one would do for quantum key distribution) and the times at which they and all necessary classical information were present at the end stations. For the purposes of this work, we focus on key rates for quantum key distribution as a familiar way to assign meaning to both the speed and quality of the entanglement distribution process. However, the simulation is not limited to this application and the obtained information can easily be used to calculate other figures of merit, such as the raw rate of distributed pairs or the fraction of pairs above a certain fidelity threshold. For the key rates in particular, we let the simulation run until a large sample (usually 10^5) has been obtained and then

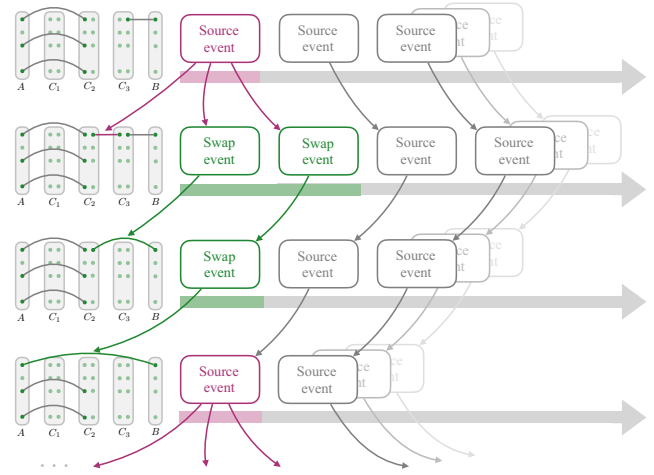


FIG. 3. An illustration of a step-by-step update of the state of the simulation and the event queue. The source event (representing the successful establishment of an entangled pair between neighboring repeater stations) triggers the protocol to schedule two new entanglement swapping events, inserting them at the front of the event queue. Resolving the entanglement swapping events establishes a long-distance pair between the end stations. After each step, i.e., after every event that is resolved, the protocol again has the chance to react to the new situation.

we use the sample mean of the error rates to estimate the asymptotic key rate.

Before moving on to the particular scenarios discussed in this work, we comment on a few design decisions of our approach. This system, centered around *events*, is very flexible when it comes to including noise models, as the events can simply be modified depending on the conditions; e.g., the repeater station from the above example may have a parameter that describes the quality of Bell-state measurements available at this particular station. *ReQuSim* supports arbitrary completely positive trace-preserving maps to describe physically meaningful noise processes.

Two key challenges that are addressed by our framework are the probabilistic nature of distributing entangled states between neighbors and the time-dependent noise that acts on qubits stored in quantum memories. In general, the probability that a photon gets lost in transmission is very high, so it is certainly not efficient to keep track of every single photon that is sent individually. Instead, we draw from a probability distribution for how many trials are needed until the next successful attempt happens (this is simply a geometric distribution if the probability of success in one trial stays constant). This means that we use a combination of two methods to handle probabilistic aspects of the simulation—a Monte Carlo approach for loss and a the density-matrix formalism for other types of noise. We handle the time-dependent nature of the noise in

quantum memories not by continuously updating the quantum state—e.g., in fixed time steps—but, instead, by doing so only when it becomes relevant; e.g., when performing an operation involving this particular entangled pair. For this, we simply need to track how much time has passed since the last time this update was performed. Both of these approaches are essential for allowing the simulation to run in a reasonable time frame.

At various points in a quantum repeater protocol, classical information needs to be exchanged. While, again, we do not simulate each individual message and are not concerned with the exact content of the classical communication, it is nonetheless essential to take the timing of classical information into account. We achieve this in our simulation by adding an appropriate delay to when an event will be able to be resolved or by blocking any additional operations being performed on a certain part of the simulation until a point in time at which the necessary classical information is able to reach the involved parties.

III. MODEL

We consider two distant parties that want to share a secret key via an entangled-swapping-based repeater protocol with one or multiple repeater stations between them. The repeater stations have the capability to locally perform quantum operations such as entanglement swapping and are equipped with quantum memories. Some of the stations also control an entangled pair source that they can use to establish entangled links between neighboring stations.

In any realistic setting, one inevitably needs to account for imperfections in multiple parts of the system, which make employing a quantum repeater protocol necessary in the first place. In the following subsections, we describe a number of sources of imperfection and how we have modeled them. Additional comments can be found in Appendix A.

A. Arrival probability

Establishing links between neighboring stations is an elementary operation for the protocols that we consider. However, creating entangled links between stations is not always successful and usually needs multiple tries.

There are sources of loss that occur systematically, regardless of the precise layout of the repeater stations. These could include, e.g., the probability of an entangled pair being generated in the first place (preparation efficiency), the wavelength-conversion efficiency, the probability that photons are successfully coupled into the optical fiber, the efficiency of the detectors, or the probability that qubits are loaded into quantum memories successfully (memory efficiency). We summarize these in an abstract success probability P_{link} , which represents the probability that a pair can be established while not taking distance-based losses into account.

Another central source of loss in the system is the distance-dependent loss of qubits during transmission. We describe this by the channel efficiency η_{ch} . For the purposes of this work, we always consider photons being sent through optical fibers but for other repeater setups (such as quantum repeaters using satellites as repeater stations), this part would need to be modified. We define

$$\eta_{\text{ch}}(L) := e^{-\frac{L}{L_{\text{att}}}}, \quad (1)$$

where L denotes the distance the photon has to travel and $L_{\text{att}} = 22$ km denotes the attenuation length of optical fibers at telecom wavelengths. Therefore, the total probability η that a pair is established between two neighboring repeater stations separated by a distance L in one trial is given by

$$\eta = P_{\text{link}} \times \eta_{\text{ch}}(L). \quad (2)$$

B. Initial fidelity

The initially created and distributed Bell pairs may also be imperfect. This could stem from an imperfect generation procedure of the entangled pair sources or from other systematic errors in the handling of the qubits of the initial pairs.

We assign an initial fidelity F_{init} , which represents all these imperfections except for the effect of dark counts, discussed in Sec. III C, which is loss dependent. The initial state given by depolarizing noise acting on the desired Bell-state vector $|\Phi^+\rangle$ is

$$\begin{aligned} \rho_{\text{init}} = & F_{\text{init}} |\Phi^+\rangle\langle\Phi^+| \\ & + \frac{1 - F_{\text{init}}}{3} (|\Phi^-\rangle\langle\Phi^-| + |\Psi^+\rangle\langle\Psi^+| + |\Psi^-\rangle\langle\Psi^-|). \end{aligned} \quad (3)$$

C. Dark counts

Dark counts are an imperfection in detectors and manifest themselves by *clicks* when no actual signal has arrived. Usually, this is measured in dark counts per second but, for our purposes, we are interested in the probability that a dark count will occur in a detection window when we would potentially expect a signal. We denote this probability by p_d , e.g., for a detector with a dark-count rate of 1 Hz and detection windows of 1 μs we obtain $p_d = 10^{-6}$.

We can model dark counts by replacing the erroneously expected qubit with a fully mixed state. In order to obtain the effective density matrix, not only do we need to consider the probability that a dark count occurred but we must set this into relation with the probability of a true click occurring in the first place; i.e., when success rates are very low, nearly every click is caused by a dark count.

The chance for a detector to click is given by

$$\eta_{\text{eff}} = 1 - (1 - \eta)(1 - p_d)^2 \quad (4)$$

and the probability that the click indicates a real event is then

$$\alpha(\eta) = \frac{\eta(1 - p_d)}{\eta_{\text{eff}}}. \quad (5)$$

Therefore, the state ρ that represents the output state of a successful attempt is affected by

$$\alpha(\eta)\rho + \frac{1 - \alpha(\eta)}{2}(\text{tr}_i\rho) \otimes \mathbb{1}^{(i)}, \quad (6)$$

where tr_i denotes the partial trace over the i th subsystem and $\mathbb{1}$ is the identity operator.

D. Memory noise

Since the usage of quantum memories is of central importance to this type of quantum repeater, time-dependent decoherence for qubits stored in them is another source of imperfection. We assume that the noise caused by this is predominantly in one direction and is described by a dephasing noise channel

$$\mathcal{E}_z^{(i)}(t)\rho = (1 - \lambda(t))\rho + \lambda(t)Z^{(i)}\rho Z^{(i)}, \quad (7)$$

with the index i marking the qubit that is stored in memory and with

$$\lambda(t) = \frac{1 - e^{-t/T_{\text{dp}}}}{2}, \quad (8)$$

where the dephasing time, T_{dp} , is a parameter specific to the quantum memory in question. Note that other imperfections of the memories, e.g., related to read-in and read-out of qubits, can be included in other parameters such as P_{link} and imperfections in the Bell measurements.

E. Imperfect Bell measurements

Entanglement swapping is the main quantum operation that needs to be performed once the repeater links have been established. Naturally, the necessary Bell-state measurement will be subject to imperfections, which we model as two-qubit depolarizing noise (acting on the qubits being measured) followed by the perfect Bell measurement. The two-qubit depolarizing noise acting on qubits i and j is given by

$$\mathcal{E}_w^{(ij)}(\lambda_{\text{BSM}})\rho = \lambda_{\text{BSM}}\rho + \frac{1 - \lambda_{\text{BSM}}}{4}(\text{tr}_{ij}\rho) \otimes \mathbb{1}^{(ij)}, \quad (9)$$

where tr_{ij} denotes the partial trace over the i th and j th subsystems and λ_{BSM} is the Bell-state measurement ideality

parameter (1 corresponds to perfect operation), which is a property of the repeater station at which the Bell-state measurement is performed.

Another common imperfection is that the measurement may only work with a certain probability, which not only reduces the reliability of the setup but can even change which swapping strategy should be used [31]. However, for the purposes of this work, we consider the Bell-state measurements to always be successful.

F. Distribution times

In the scenarios considered in this work, the entangled pair sources are always located directly at a repeater station S . A trial to establish an entangled pair for a repeater link is done by first creating an entangled pair, which takes a preparation time T_P (in practical terms, this is often related to the clock rate f_{clock} of the entangled pair source). After one of the qubits is loaded into the memory at station S , the other qubit is sent to a neighboring station S' . Before any part of the entangled pair can be used, S needs to wait for a classical message from station S' confirming whether the qubit arrived successfully. Therefore, one trial will take $t_{\text{trial}} = T_P + 2d/c$, where d is the distance between S and S' and $c = 2 \times 10^8$ m/s is the speed of light in optical fiber.

This also means that when the pair is confirmed to be successfully established, the qubit at S will already have been affected by memory noise for a duration of $2d/c$ and the qubit at S' for d/c .

Since loss is a major source of imperfection, it is highly likely that multiple trials are needed to establish an entangled state between neighboring stations. If the trial is not successful, the qubit in memory needs to be discarded and the process started again from the beginning. The time it takes until the next entangled pair is established can be obtained by

$$k \times t_{\text{trial}}, \quad (10)$$

where k is drawn randomly from a geometric distribution $k(\eta_{\text{eff}})$ with a success probability η_{eff} . Note that both t_{trial} and η_{eff} are distance dependent.

In scenarios with multiple memories, we assume that the trials are performed simultaneously and independently for each memory slot. For simplicity, we treat them as using spatially separate channels, although in practice one would likely need to consider allocation of certain time slots in the quantum channel to specific processes. However, as long as the time of one trial is much larger than the time it takes to prepare a new entangled pair for sending, any effects arising from this are very small.

IV. RESULTS AND DISCUSSION

At the core of an entanglement-swapping-based quantum repeater protocol (as opposed to a scheme using

quantum error correction instead [19]) lies the realization that subdividing a channel into multiple parts and using entanglement swapping can be beneficial. However, many previous investigations fall roughly into two very different categories. On the one hand, there are very abstract models that presume that a large ensemble of entangled states is readily available at the lowest repeater level and that the main source of imperfections is the (potentially distance dependent) fidelity of these initial states, while the quantum memories are of very high quality and the use of entanglement purification protocols is plentiful (see, e.g., Refs. [7,8,32,33]). In these kinds of scenarios, choosing the number of purification steps at each repeater level is the main challenge in optimizing the protocols.

On the other hand, there are models that are closer to the experimental setups (see, e.g., Refs. [9,22,23,34]), where loss of qubits during the initial distribution of entangled states is a major factor and the coherence times of memories are rather short—and entanglement purification is hardly considered, if at all. Instead, the focus of the analysis is to take into account the exact timing of the qubits arriving and the operations being performed. Remarkably, the basic approach of shorter channel segments and entanglement swapping has proved useful in these very different situations.

A. Two links with entanglement purification

In the following, we investigate a situation that can be seen as being located somewhere in between the two categories mentioned above: quantum repeater protocols using entanglement purification while properly considering the timing considerations in the presence of realistic error models.

It is easy to see the pros and cons of adding entanglement purification when considering the extreme ends of the parameter regime. If the initially generated entangled states are of such low fidelity that after performing entanglement swapping the output state is no longer useful (e.g., it would introduce a too high quantum bit error rate for key distribution or fall short of some threshold fidelity at the output), no meaningful connection can be established without a mechanism to improve the fidelity. Entanglement purification protocols can help in this case by increasing the fidelity above the relevant threshold, if the quality of the quantum memories is sufficiently high to accommodate the additional time needed to perform them. However, if the decoherence time of the quantum memories is very short, clearly any gain in the fidelity from entanglement purification will be long gone by the time the required classical information arrives and, therefore, performing entanglement swapping as soon as possible is more desirable.

Here, we investigate parameters in between those extremes and especially initial fidelities F_{init} for which both

approaches—with and without the use of an *entanglement purification protocol* (EPP)—can, in principle, achieve nonzero key rates. This allows us to quantify under which circumstances the use of EPPs can be beneficial in this intermediate regime and what memory times need to be achieved in order to make that possible. A similar perspective on the trade-off between using additional memories for entanglement purification or multiplexing has been studied in Ref. [35], albeit with perfect quantum memories.

For now, consider a setup with a single repeater station, i.e., one consisting of two repeater links. The repeater station is equipped with an entangled pair source and four memories per repeater link, so multiple pairs can potentially be established simultaneously. Zero, one, or two steps of the DEJMPS entanglement purification protocol [36] (see also Appendix A 1) are performed on each side before the station applies entanglement swapping. The established connections are then used to perform quantum key distribution. However, entanglement purification is a probabilistic process and measurement outcomes have to be communicated between the involved parties in order for them to know whether the EPP has been successful.

If no entanglement purification is performed, the end stations do not need to have quantum memories, because the arriving qubits can be measured right away. However, when performing entanglement purification, the end stations will also need to be equipped with quantum memories. Since in this instance we are only concerned about the secret key rate and not about storing a final long-distance entangled state, at the end stations the output qubits of the final EPP step can be measured immediately to avoid additional time in memory, even though the classical information about whether the entanglement purification was successful has not arrived yet.

In Fig. 4, the achievable key rates with a varying number of entanglement purification steps are shown for a selection of specific values of F_{init} , for which the use of entanglement purification is just barely advantageous. For the given parameters, at $F_{\text{init}} = 0.95$ the use of entanglement purification actually leads to a slight reduction in the achievable key rate for most distances (e.g., key rates of approximately 61 Hz with one step of EPP compared to approximately 75 Hz without EPP at 100 km). However, the use of an EPP can extend the distances for which a positive key rate can be achieved by a bit (from approximately 160 km to approximately 170 km), because there the reduction in error rate by the EPP is actually worth the lower raw bit rate. As expected from the extreme parameter regimes discussed above, if F_{init} is sufficiently low, the use of entanglement purification is indeed just outright beneficial (as is the case in Fig. 4(b) with $F_{\text{init}} = 0.935$).

For both of these cases, it is also clear that doing more than one step of entanglement purification is not helpful. However, more purification steps may become useful at even lower F_{init} . In any case, clearly, the number of

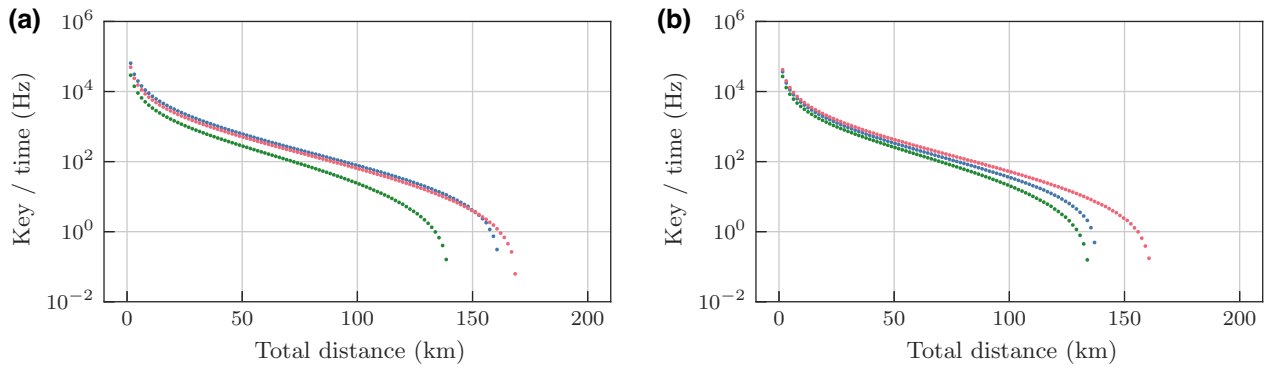


FIG. 4. The obtainable key rates for two repeater links with zero (blue), one (red), or two (green) entanglement purification steps before entanglement swapping. (a) $F_{\text{init}} = 0.95$. Even though no *entanglement purification protocol* (EPP) is necessary for most distances, an EPP can help to extend the reachable distance. (b) $F_{\text{init}} = 0.935$. At worse initial fidelity, an EPP can improve the key rate for all distances. In both cases, it is also apparent that the number of purification steps needs to be managed carefully. For these parameters, using two purification steps is actually detrimental. The other parameters are as follows: $T_{\text{dp}} = 100$ ms, $P_{\text{link}} = 0.5$, and $p_d = 10^{-6}$, with four memories per repeater link.

purification steps to be performed as part of the protocol needs to be carefully adjusted according to which experimental parameters are available.

We remark that in order to optimize this even further, other schemes of entanglement purification could be considered. For example, a pumping scheme [37] could be employed instead of a strict repetition scheme. Alternatively, the number of entanglement purification steps could be dynamically adjusted depending on whether or not the other link was already ready for entanglement swapping.

While the above examples demonstrate that there are situations for which the use of EPPs is worth considering, in Fig. 5 a wider range of parameters is considered. The figure shows the increase in the reachable distance, i.e., where a nonzero key rate can still be achieved, when using one EPP step compared to not using entanglement purification. As expected, the addition of entanglement

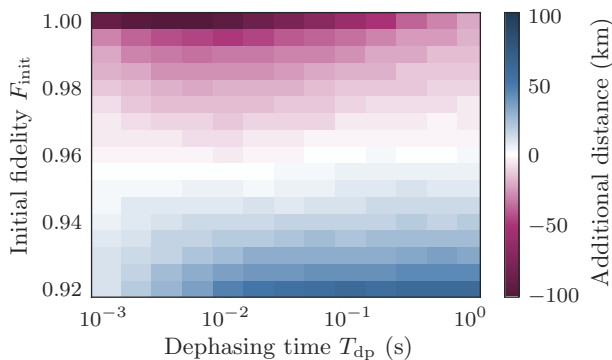


FIG. 5. The increase in the achievable distance (i.e., with a nonzero key rate) using a repeater protocol with one entanglement purification step compared to a repeater protocol without entanglement purification. The other parameters are as follows: $P_{\text{link}} = 0.5$ and $p_d = 10^{-6}$, with four memories per repeater link.

purification is most impactful when F_{init} is low and the memory quality (represented by the dephasing time T_{dp}) is high. However, the figure also shows that the usefulness is not restricted to the most extreme cases but that the addition of entanglement purification can somewhat extend secure transmission distances for a wide range of parameters.

1. Cutoff time as an alternative strategy

In essence, the use of entanglement purification can be understood as one way of trading some of the raw rate for a higher fidelity of the pairs that are used. However, another strategy that is also reducing the raw rate in exchange for a lower error rate is simply discarding qubits that have been kept in storage for too long. A common mechanism for this is to choose a fixed cutoff time t_{cut} (see, e.g., Ref. [38]) after which a qubit is discarded and the process of establishing a link is started again. In general, optimizing whether to keep or discard an existing link has been shown to be exponentially hard [39], since all decisions at previous times need to be taken into account as well to formulate the optimal strategy. However, at the individual link level, a cutoff-time strategy is indeed optimal in the steady-state limit [40].

We have applied the cutoff-time approach both for the protocol with and without EPP for an F_{init} that is just barely above the threshold at which a non-EPP protocol is viable. A selection of the best cutoff times that we have found for both approaches is shown in Fig. 6. First, it shows that the EPP approach can also benefit from some upper limit on the storage time. Naturally, the optimal cutoff time is much higher for the entanglement purification approach, as one must allow time for the classical information after the entanglement purification as well. This demonstrates that one necessarily needs to consider combinations of

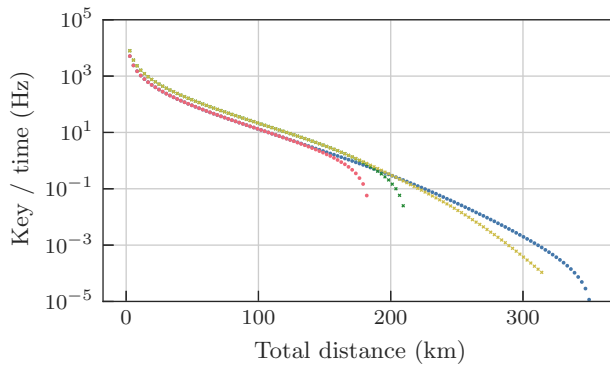


FIG. 6. The achievable key rates for two repeater links with a combination of strategies, without entanglement purification and with cutoff times $t_{\text{cut}} = \infty$ (red) or 50 ms (blue). Alternatively, a protocol with one step of entanglement purification and cutoff times $t_{\text{cut}} = \infty$ (green) or 650 ms (yellow). Properly optimized cutoff times can clearly help in both cases. The other parameters are as follows: $T_{\text{dp}} = 1$ s, $P_{\text{link}} = 0.5$, and $F_{\text{init}} = 0.925$, with two memories per repeater link.

approaches when designing quantum repeater protocols. Furthermore, this shows that the trade-off between the EPP and cutoff-time strategies is complex: for short distances, the use of entanglement purification leads to higher key rates; however, the simple protocol without entanglement purification (but with optimized cutoff times) is the better choice at long distances for this parameter set.

Even though entanglement purification and cutoff times are used for similar reasons, it should be noted there is a fundamental difference between them. While cutoff times can reduce the effect of decoherence on the final states, it cannot increase the fidelity of an individual state. For even lower F_{init} , where using a method to increase the fidelity of a pair (like EPPs) is necessary, simply optimizing the cutoff time cannot be sufficient.

B. Multiple repeater links

A single repeater station is already very useful in reaching longer distances and allows the fundamental limits of repeaterless quantum communication to be overcome. However, with the increasing loss over distance, invariably one will need to consider adding more repeater stations at some point, e.g., the exponential loss in optical fibers is a severe limitation when aiming for intercontinental distances. Indeed, the multiple-station scenario is where the quantum memories truly become indispensable, as for a single station so-called twin-field QKD [41] achieves repeaterlike scaling with only a simplified relay station that can perform measurements but has no memories.

In principle, subdividing a channel into more segments is very attractive. After all, if adding in a repeater station can improve the connection between two parties under certain conditions, it stands to reason that the same

principle can be applied for each individual link. For each individual segment, the channel loss in much shorter connections will be lower. Naturally, this does not come without a trade-off: all the imperfections that are not distance dependent but, instead, are related to generation of the entangled states, handling the states, and performing operations will be present at each of these repeater links, therefore affecting the output multiple times. In order to optimize the connection between two distant parties, the number of repeater links is an additional factor to consider and will certainly depend on the parameters of the available quantum hardware.

For repeater setups with multiple repeater links (without entanglement purification), some expressions for average waiting times are known, e.g., with probabilistic entanglement swapping [22,34,42] or for specific loss models, e.g., suited for satellite-based repeaters [43]. For some setups, even expressions for the obtainable key have been found recently [24].

To investigate the inherent trade-off when adding the additional repeater stations mentioned above, we opt for a simple model of fixed per-link overhead. We consider an imperfect initial fidelity, $F_{\text{init}} < 1.0$, of the generated entangled states at each repeater link. This could be interpreted as either imperfect entangled pair sources or some additional constant imperfections that arise from handling the states at the repeater station, e.g., by the read-in procedure that loads an arriving qubit into the quantum memory. One could also consider different sources of imperfections that happen at every link, such as imperfect operations to perform Bell-state measurements at the repeater stations (which has an effect similar to lowering F_{init}), or even a combination of multiple noisy processes. However, we focus on a single parameter for now, in order to keep the results easier to interpret. Furthermore, we limit our investigation to an equidistant spacing of repeater stations, although this may not be optimal in some cases, e.g., when photons cannot be sent in both directions simultaneously [9], and asymmetric repeater setups come with their own set of considerations (see, e.g., Ref. [44]). In Fig. 7(a), perfect initial states ($F_{\text{init}} = 1.0$) with multiple repeater stations are considered. While there are still some factors to consider that arise from using multiple repeater stations, such as many qubits potentially dephasing in quantum memories at multiple stations, the addition of more repeater links is generally favorable. For example, at approximately 150 km, key rates are improved by a factor of approximately 30, 260, 1100, or 3500 when using 4, 8, 16, or 32 repeater links, respectively, compared to a two-link approach.

However, adding even a tiny constant overhead per repeater link immediately demonstrates that there is a serious trade-off when adding more repeater stations, as is apparent from Fig. 7(b) with $F_{\text{init}} = 0.998$. It also clearly illustrates that the optimal number of repeater stations can

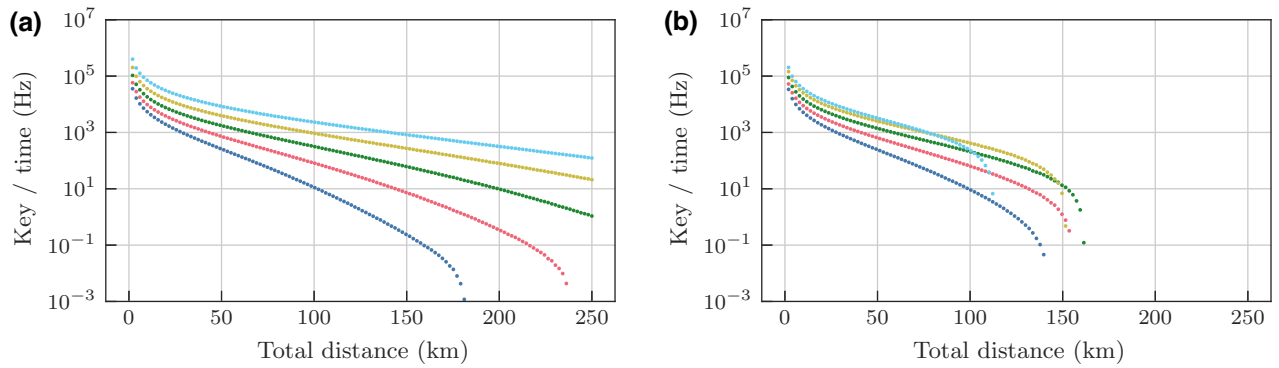


FIG. 7. The obtainable key rates when using protocols with two (blue), four (red), eight (green), 16 (yellow), or 32 (cyan) repeater links. (a) With $F_{\text{init}} = 1.0$, the utilization of more repeater links is generally favorable. (b) Even with small constant overheads per repeater link ($F_{\text{init}} = 0.998$), trade-offs become apparent. The other parameters are as follows: $T_{\text{dp}} = 10$ ms, $P_{\text{link}} = 0.5$, and $p_d = 10^{-6}$.

be different depending on the distance between the end stations; e.g., for these parameters, using a protocol with 32 repeater links leads to improved key rates at 50 km distance but the protocol with eight repeater links allows us to reach much greater distances overall.

Naturally, the point at which adding more repeater stations becomes detrimental depends strongly on the per-link overhead itself. When looking at different values of F_{init} in Fig. 8, we can see that making efforts to improve an experimental parameter can have implications beyond simply increasing achievable rates for a fixed strategy. For example, when considering end stations 125 km apart for this particular set of parameters, improving the achievable F_{init} allows us to switch to using a protocol with more repeater

links that increases the obtainable key rate even more than the F_{init} improvement alone would have done.

This demonstrates that considering multiple different repeater strategies is vital when analyzing quantum communication setups. Even if more complex schemes are not realistically possible at present, if improved operations or devices are likely to exist in the future, it might open possibilities for new strategies. Furthermore, this example illustrates how simulation tools can potentially guide experimental developments. Being able to quantify the effect of improving a certain experimental parameter is essential in making an informed decision on where to focus future efforts.

1. Entanglement purification at the lowest level

When considering entanglement purification as an additional tool for repeater protocols with multiple links, many variations of protocols are possible (e.g., an approach that is generally similar but differs in detail is analyzed in Ref. [25]). This is because, in principle, one can apply entanglement purification protocols at multiple points of the whole process, e.g., after a certain number of swapping operations it can even become essential to improve the fidelity of the entangled pair via entanglement purification lest the system becomes completely disentangled. In fact, due to the relative increase in fidelity of repetition protocols being dependent on the input states, on which repeater levels to put the entanglement purification steps has been a consideration for entanglement-swapping-based quantum repeaters from the very beginning [7,8]. However, with coherence times of quantum memories remaining a central limitation for the foreseeable future, it remains doubtful how useful entanglement purification at higher repeater levels can be. One entanglement purification step at that level is costly in terms of resources, as for the creation of each of the long-distance pairs, multiple lowest-level pairs have been used. Furthermore, with the increasing distance at higher repeater levels, the transmission of the

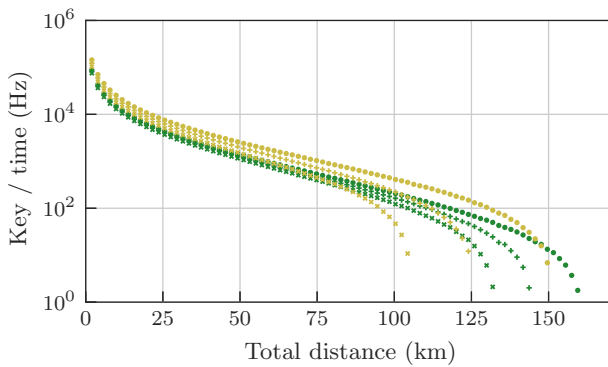


FIG. 8. Key rates for eight (green) or 16 (yellow) repeater links, with varying initial fidelities: $F_{\text{init}} = 0.996$ (crosses), 0.997 (plus signs), or 0.998 (circles). Improving some experimental parameters can enable alternative strategies. For example, when connecting end stations 125 km apart, improving F_{init} from 0.996 to 0.998 allows changing from an eight-link protocol to a 16-link protocol, which improves the obtainable key rate more than the increase in F_{init} alone. The other parameters are as follows: $T_{\text{dp}} = 10$ ms, $P_{\text{link}} = 0.5$, and $p_d = 10^{-6}$.

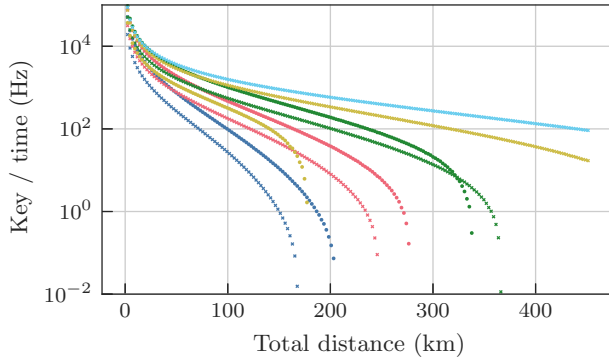


FIG. 9. Entanglement purification can extend achievable ranges for quantum repeaters with multiple links. Key rates without entanglement purification (circles) and with one step of entanglement purification at the lowest level (crosses) when using two (blue), four (red), eight (green), 16 (yellow), or 32 (cyan) repeater links. The parameters are as follows: $T_{\text{dp}} = 100$ ms, $F_{\text{init}} = 0.99$, $P_{\text{link}} = 0.5$, and $p_d = 10^{-6}$, with two quantum memories per repeater link at each station.

classical information necessary for performing the entanglement purification protocol will take longer and at some point the increase in fidelity achieved through an entanglement purification protocol will be negated by the noise processes in the memory during this time.

Optimizing repeater protocols with entanglement purification in mind therefore inevitably means considering these complex trade-offs. For the purpose of this work, we only consider whether adding entanglement purification at the lowest level, i.e., purifying only the initial entangled pairs distributed to neighboring repeater stations, can already be beneficial.

We consider a setup with high-quality memories ($T_{\text{dp}} = 100$ ms), which favors entanglement purification, and analyze the question of whether one step of entanglement purification at the lowest level should be performed. The results are depicted in Fig. 9; they show that for this parameter set, entanglement purification significantly changes the impact of the trade-offs being made when including additional repeater stations. In fact, it is what makes using more repeater stations viable in this case, which in turn improves the reachable distances significantly. This is one example of how the use of entanglement purification can be beneficial not just when considering very low initial fidelities but even when dealing with initial states with relatively high F_{init} . More generally, it showcases how access to certain tools (such as entanglement purification) makes it necessary to reevaluate other aspects of how the repeater setup is constructed.

C. Impact of improving parameters for custom error models

For the previous results, we have used a fairly uniform error model to make the results easy to interpret. In order to

showcase a broader range of error models, we consider an alternative noise model and analyze the effect of improving certain parameters of the hardware. This also follows the line of thought of the previous scenario that a small change in conditions can have a significant effect on the overall outcome.

We consider quantum memories with a time-dependent amplitude damping channel captured as

$$\mathcal{E}_{\text{damp}}^{(i)}(t)\rho = \begin{pmatrix} 1 & 0 \\ 0 & \sqrt{1-\gamma(t)} \end{pmatrix} \rho \begin{pmatrix} 1 & 0 \\ 0 & \sqrt{1-\gamma(t)} \end{pmatrix} + \begin{pmatrix} 0 & \sqrt{\gamma(t)} \\ 0 & 0 \end{pmatrix} \rho \begin{pmatrix} 0 & 0 \\ \sqrt{\gamma(t)} & 0 \end{pmatrix}, \quad (11)$$

with $\gamma(t) = 1 - e^{-t/T_{\text{damp}}}$ and the damping time T_{damp} . Furthermore, we assume that both entanglement purification and Bell-state measurements are performed in a gate-based way with the same two-qubit gate error parameter p_{gate} . The noisy controlled-NOT (CNOT) gates involved in both of these operations are modeled as local depolarizing noise channels $\mathcal{E}_d(p_{\text{gate}})$ acting on both of the input qubits, followed by the perfect gate operation. The local depolarizing channel on the i th qubit is defined as

$$\mathcal{E}_d^{(i)}(p_{\text{gate}})\rho = p_{\text{gate}}\rho + \frac{1-p_{\text{gate}}}{2}\text{tr}_i(\rho) \otimes \mathbb{1}^{(i)}, \quad (12)$$

with tr_i denoting the partial trace over the i th subsystem.

In Fig. 10, the impact of making improvements to either the memories (higher T_{damp}) or the two-qubit gates (higher p_{gate}) on the reachable key rate is shown for a protocol with four repeater links and one entanglement purification step at the lowest level. It is clear that both parameters have strict minimum requirements to achieve a nonzero key rate with this protocol at a specified distance.

V. RELATED WORK

In recent years, many tools have been released to study various aspects of quantum repeaters and quantum networks. Naturally, each of them focuses on a different aspect of quantum communication and uses differing assumptions and abstractions to model what is important for its specific considerations. Such a variety of interpretations and implementations is certainly beneficial to the discussion in the field and the overall understanding of quantum networks. At the same time, the field of quantum network simulation is not really mature enough to have a standardized framework for comparing features and protocols. In the following, we give a brief overview of some of the available simulation platforms.

SimulaQron [45] provides a distributed classical simulation of multiple connected parties with quantum computers that allows us to use the delay of real-world classical networks as part of its model. Furthermore, it allows

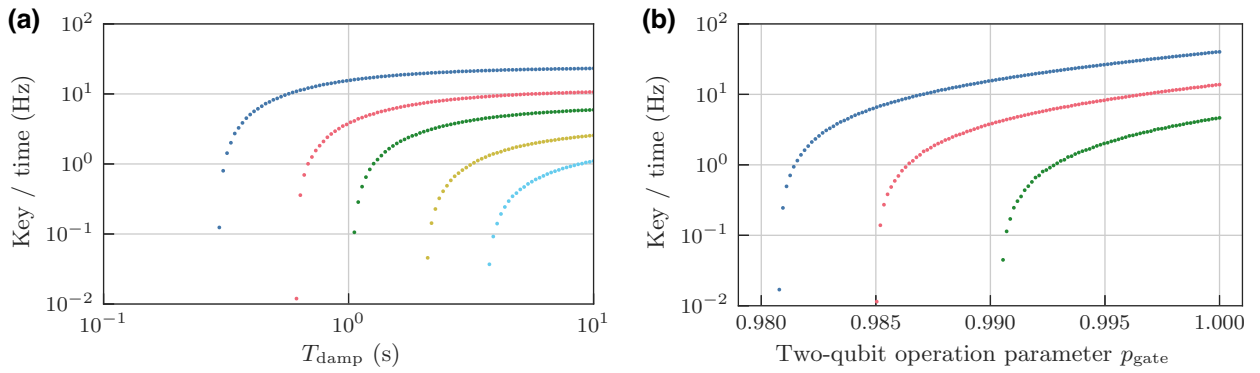


FIG. 10. The impact of improving certain hardware parameters for a custom error model, using a repeater protocol with four repeater links and one entanglement purification step at the lowest repeater level. Two quantum memories per connected link are available at each station. The parameters are as follows: $P_{\text{link}} = 0.01$, $p_d = 10^{-6}$, and $F_{\text{init}} = 0.99$. For a total distance of 20 (blue), 35 (red), 50 (green), 75 (yellow), or 100 (cyan) km: (a) varying memory quality with a fixed $p_{\text{gate}} = 0.99$; (b) varying quality of two-qubit gates with fixed $T_{\text{damp}} = 1$ s (no positive key rate for 75 or 100 km).

the development of software for quantum networks based on the instruction set architecture *NetQASM* [46], which would then allow the protocols that were built using the simulation to be run on quantum hardware.

QuISP [26] uses an event-driven approach to simulate quantum networks but it places a much stronger focus on the networking aspects for large-scale networks. It achieves the necessary scalability by updating an error model rather than tracking full quantum states.

Close in mindset to the approach introduced in this work are the approaches followed by *NetSquid* [25] and *SeQeNCe* [27], which are both event-based software tools for modeling and simulating quantum networks. *NetSquid* has also been used in the context of quantum repeater chains with realistic hardware. In Ref. [25], a setup with a different variation of an entanglement purification strategy is analyzed for a NV-center-based quantum repeater stations with additional hardware restrictions. It has also been used to consider aspects for quantum repeaters based on atomic ensembles [47] and real-world fiber infrastructure [28], as well as the use of genetic algorithms to optimize repeater protocols [29,48]. *SeQeNCe* has investigated the distribution of entangled states in a nine-node network in Ref. [27]. It has also been used to model and analyze a specific generation procedure for photonic quantum states with absorptive quantum memories [49]. In Ref. [50], it is explained how the simulator can parallelize some calculations.

VI. SUMMARY AND OUTLOOK

Quantum communication constitutes a central pillar of quantum technologies, with cryptographic applications being the main practical application. The vision of achieving secure communication over arbitrary distances requires overcoming the strict limitations that stem from not having

quantum repeaters available. Hence, the quest for achieving realistic and efficient quantum repeater protocols is by no means a detail but is actually a core step before practically relevant protocols of quantum communication over arbitrary distances become viable. Research on hardware development is progressing well but has to confront the situation that the multitude of design rules renders the optimal construction of quantum repeaters challenging.

In order to substantially assist this task, we have developed a numerical simulation that allows us to analyze practical quantum repeater setups, as a versatile scheme, but one that is sufficiently detailed that a multitude of physical aspects can be accommodated. We stress that our approach can obtain not only waiting times but also calculate quantities directly from the output distribution (such as secret key rates) while taking into account the probabilistic distribution of initial states, time-dependent memory noise, multiple quantum memories per repeater link, entanglement purification, and multiple repeater links (including analyses for up to 32 in this work and a demonstration of up to 1024 in Appendix B).

We have analyzed multiple scenarios that are focused on the comparison and combination of repeater strategies: we have explored the use of entanglement purification as part of a quantum repeater protocol and quantified under which circumstances employing such a strategy can be beneficial. More importantly, we have found that increasing the complexity in this way may be unwarranted if a strategy with optimized cutoff times can produce similar or even greater performance. Furthermore, we have analyzed the trade-offs that come with protocols that use multiple repeater links and provided a clear example of how improving the experimental capabilities (e.g., better initial fidelities) can make new options for optimization (e.g., using more repeater stations) viable, which leads to a larger improvement overall than would be obtainable in isolation.

In general, there are a multitude of questions when it comes to the design of quantum repeaters or, at a higher level, quantum networks. One of the main challenges in exploring further options is that the parameter space is not only vast but any result of optimality can only be understood in a specific context and with a specific set of tools in mind. While our approach will certainly allow us to explore different parameter regimes in a more rigorous manner, we expect that it will be particularly useful for investigating advanced repeater protocols, e.g., for asymmetric setups or with dynamic adjustments of strategies. Another possible direction is to use a numerical simulation to closely model particular experimental setups and investigate the viability of building more complex schemes with currently available experimental hardware (e.g., Ref. [28] follows such an approach). It is the hope that the versatile platform presented here will contribute substantially to the quest of identifying good design principles for feasible quantum repeaters and hence contribute to achieving quantum communication over arbitrary distances.

The simulation framework *ReQuSim* [30] is available as an open-source PYTHON package. The code that has been used to generate all of the results presented in this work is archived at Ref. [51]. It uses a combination of *ReQuSim v0.4* and an earlier version of the code base that has not been released as a stand-alone package. The raw output data of the simulation that has been used to calculate the values presented in the plots is available upon reasonable request.

ACKNOWLEDGMENTS

J.W. and J.E. acknowledge support from the Federal Ministry of Education and Research (BMBF) via projects Q.Link.X and QR.X. F.W. and F.H. acknowledge support from the German Research Foundation (DFG) under the Emmy Noether program via Grant No. 418294583. N.W. and J.E. acknowledge support from the BMBF via the projects PhoQuant and QPIC-1. J.E. also thanks the European Research Council (DebuQC) for support. We thank the High-Performance Computing (HPC) Service of Die Zentraleinrichtung für Datenverarbeitung (ZEDAT) [52], the Freie Universität Berlin, and the HPC Service of the Department of Physics, Freie Universität Berlin, for computing time.

APPENDIX A: MODELS AND EVALUATION

In general, the notation and underlying models used in this work are derived from those of Refs. [9,21,23] (the scenarios considered in Appendix C) but adapted in a way that fits all of them into one coherent style. Here, we comment on a few additional details of our model and strategies.

1. Entanglement purification

Entanglement purification protocols are a class of quantum protocols using only *local operations and classical communication* (LOCC) to (potentially probabilistically) transform multiple copies of a noisy entangled state into fewer copies of the same states with a higher fidelity. They are one strategy to deal with the noise and imperfections that inevitably arise in any realistic scenario.

In this work, we use the DEJMPS EPP [36]. It is a probabilistic protocol for purifying $|\Phi^+\rangle$ state vectors, taking two noisy states, ρ_{A_1, B_1} and ρ_{A_2, B_2} , as input. On both copies, $\sqrt{-iX} \otimes \sqrt{iX}$ is applied, before applying a multilateral CNOT operation $\text{CNOT}^{A_1 \rightarrow A_2} \otimes \text{CNOT}^{B_1 \rightarrow B_2}$ and measuring the second pair in the computational basis. The protocol is considered successful if the measurement outcomes coincide; otherwise, it is unsuccessful and the remaining pair has to be discarded. If the initial fidelity of the input states is sufficiently high, a repeated application of this protocol will result in an increased fidelity for the output pair.

As an example, consider the base case of two input pairs in the same state ρ , which is diagonal in the Bell basis with coefficient λ_{ij} . If the desired state vector $|\Phi^+\rangle$ is affected by local Pauli-diagonal noise, it will always be diagonal in the Bell basis. As a side note, an arbitrary bipartite state can be brought into this form by probabilistic application of operations (see, e.g., Ref. [53]); however, this is not necessary for the protocol to function, as off-diagonal entries do not affect the protocol adversely [36]. We write

$$\rho = \lambda_{0,0} |\Phi^+\rangle\langle\Phi^+| + \lambda_{1,0} |\Phi^-\rangle\langle\Phi^-| + \lambda_{0,1} |\Psi^+\rangle\langle\Psi^+| + \lambda_{1,1} |\Psi^-\rangle\langle\Psi^-|. \quad (\text{A1})$$

The effective map after a successful entanglement purification step is given by

$$\begin{aligned} \tilde{\lambda}_{0,0} &= \frac{\lambda_{0,0}^2 + \lambda_{1,1}^2}{N}, & \tilde{\lambda}_{1,0} &= \frac{2\lambda_{0,0}\lambda_{1,1}}{N}, \\ \tilde{\lambda}_{0,1} &= \frac{\lambda_{0,1}^2 + \lambda_{1,0}^2}{N}, & \tilde{\lambda}_{1,1} &= \frac{2\lambda_{0,1}\lambda_{1,0}}{N}, \end{aligned} \quad (\text{A2})$$

with $N = (\lambda_{0,0} + \lambda_{1,1})^2 + (\lambda_{0,1} + \lambda_{1,0})^2$ as a normalization constant that is also the probability of success.

If the initial fidelity $\lambda_{0,0}$ is sufficiently high, a repeated application of this protocol will result in an amplification of that coefficient. In Ref. [36], this repeated application is formulated as a repetition protocol; i.e., one performs the above protocol on many initial copies and uses the output copies of successful purification steps as input for the second step.

In the scenarios considered in this work, it is common that the input pairs used for the DEJMPS protocol are not identical. If one pair has been established between two parties, it will often have to wait in noisy quantum memories

until a second pair can be established and the entanglement purification protocol can be performed. In the context of a quantum repeater, it is also important to stress the necessity of communicating the measurement outcomes, which need to be communicated to both parties performing the protocol in order to decide whether the entanglement purification was successful.

2. Key rates

The *asymptotic key rate* (per time) is lower bounded by [9,54,55]

$$r[1 - h(e_x) - fh(e_z)], \quad (\text{A3})$$

where r is the raw rate of bits obtained from measurements at the end stations that have been confirmed to correspond to successful entanglement swapping operations at the repeater stations, h is the binary entropy function, and $e_{X(Z)}$ represents the quantum bit-error rate of measurements in the X (Z) basis. Furthermore, the key rate can be constrained by an error correction inefficiency $f \geq 1$, with 1 being the ideal case.

In this work, we obtain a large sample of long-distance links between the end stations of the repeater chain from our simulation and use the sample mean of r and $e_{X(Z)}$ to calculate an estimate for the asymptotic key rate (A3). However, it should be noted that in practice, the effects of finite-size effects should be carefully considered for cryptographic applications [56]; e.g., some special considerations for satellite-based quantum key distribution (because of the small expected block sizes for current experimental parameters) are discussed in Refs. [57,58].

It should be noted that the term “key rate” is used for multiple related quantities in the literature. Some publications instead focus on the key rate per channel use, with the yield Y instead of the raw rate r . Furthermore, some use $Y/2$ or $r/2$ to obtain a key rate per mode, since the B92 protocol [59] requires two modes. It is also worth mentioning that depending on how the channel uses are counted, the key rate per time may either be directly related to the key rate per channel uses (if the potential number of channel uses in a time interval is counted) or not directly related; e.g., if the actual number of photons sent through a channel in a sequential protocol is counted.

APPENDIX B: SCALING TO MORE REPEATER LINKS

The main text is restricted to discussing setups of up to 32 repeater links, which is both due to using models that are straightforward to interpret but also because, as Sec. IV B clearly shows, the range of scenarios that are both viable and interesting while using the same parameter sets is inherently limited.

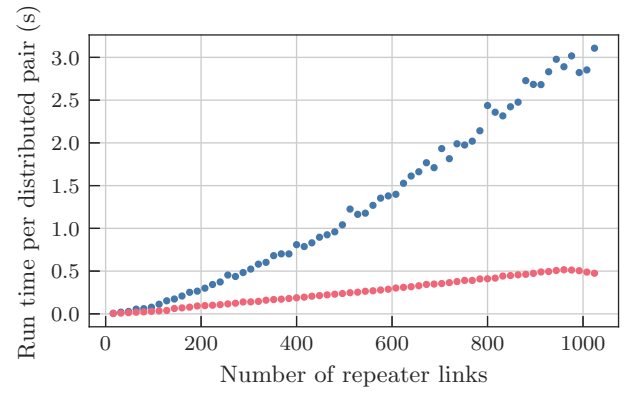


FIG. 11. The scaling of the run times of the simulation with the number of repeater links. This is for a setup with single memories and no entanglement purification, as in Sec. IV B. Two methods of scheduling events are compared: a general adjustable method indicative of the protocols used in the rest of this work (blue) and a specialized one for this scenario optimized for scaling (red).

In Fig. 11, the run times of repeater setups up to 1024 repeater links are shown. These have been obtained on a machine with an Intel Core i9-12900 processor, running up to six data points in parallel.

APPENDIX C: KNOWN SETUPS WITH ANALYTICAL RESULTS

As part of developing the simulation, we have naturally tested our approach using known analytical results. In the following, we use the error models and protocols from some specific publications and recreate them using our simulation. We have done this not only to test whether our simulation works correctly but also to show that our simulation can support the kind of error models frequently found in the literature. Our framework goes substantially beyond the first steps that have been taken toward the simulation of repeaters in Ref. [60], on which this comprehensive simulation platform presented here builds.

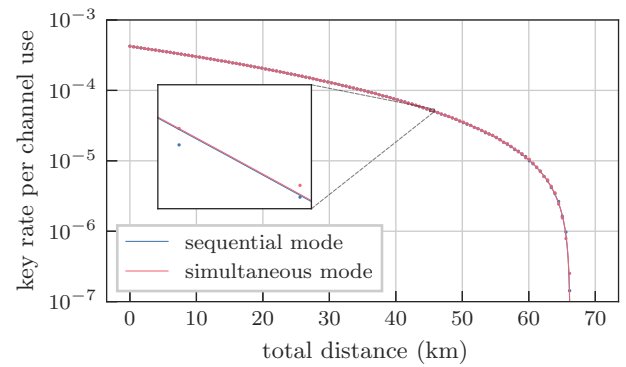


FIG. 12. The obtainable key rates for the two-link repeater protocol and parameters described in Ref. [9]. A comparison of the analytical formulas (lines) and our simulation (dots).

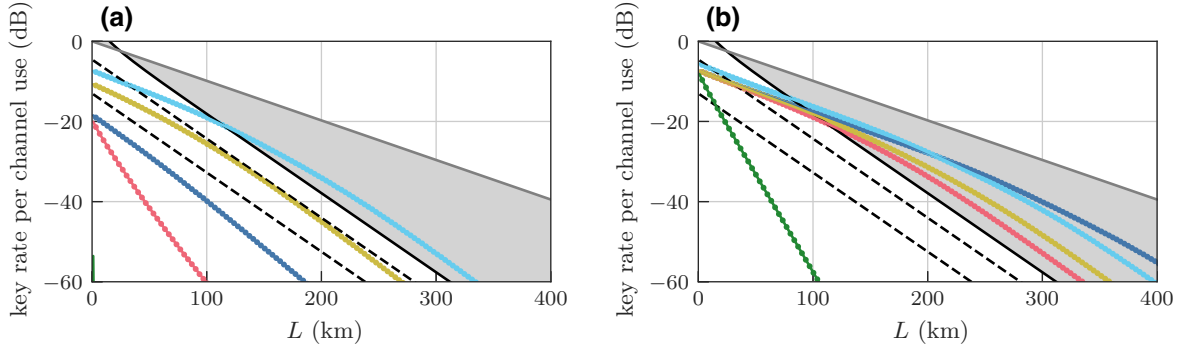


FIG. 13. Key rates for node-sends-photons protocols with (a) currently available or (b) future parameters. The experimental platforms are NV centers (dark blue), silicon-vacancy (SiV) centers (red), Quantum dots (green), Ca or Yb ions (yellow), and Rb atoms (light blue), with parameters taken from Ref. [21]. A comparison of the analytical formulas (lines) and our simulation (dots). The solid black line is the PLOB bound and the solid gray line represents $\sqrt{\eta}$ (the asymptotic behavior and upper bound [61] of the ideal one-repeater setup). The two dashed lines are $P_{\text{link}}\eta/2$ for $P_{\text{link}} = 0.7$ and 0.1 .

In the following, we will briefly describe the protocols, explain how the error model translates to our parameter set, and show that our numerically calculated key rates agree with the analytical formulas. All of them use a key rate per channel use as a metric.

1. Memory-based quantum repeater with two links

In Ref. [9], a generic repeater protocol with one repeater station is analyzed. Entangled pairs are created at the repeater station with one qubit directly loaded into the memory, while the other is sent via glass fiber to the end stations. There are two variants of this protocol, one with sequential entanglement generation—i.e., first only one of the sides tries to establish an entangled pair and only after that is successful is the process started for the other side—and a simultaneous variant, where both sides are trying to establish pairs simultaneously.

This scenario has an additional parameter for the imperfection that arises from the setups of different repeater stations being misaligned. This can be modeled as a Y -noise channel with misalignment error, $e_{\text{ma}} \in [0, 1]$, acting

on one of the qubits:

$$\mathcal{D}_Y^{(i)}(e_{\text{ma}})\rho = (1 - e_{\text{ma}})\rho + e_{\text{ma}}Y^{(i)}\rho Y^{(i)}, \quad (\text{C1})$$

where \mathcal{D}_Y denotes the Pauli- Y -noise channel and Y is the Pauli- Y operator, with the superscript (i) indicating that they each act on the i th qubit. Note that a Y -noise error is consistent with a symmetric randomly distributed misalignment angle of the detectors for photonic polarization-encoded qubits for measurements in the X - Z plane. Both the BB84 and B92 QKD protocols, as well as the Bell-state measurements for entanglement swapping, rely on these measurements in the X - Z plane.

In Fig. 12, the results of our simulation are shown compared to the analytical formulas (cf. Ref. [9, Fig. 3]). The parameters for this scenario are as follows: $P_{\text{link}} = 0.002376$, $T_P = 2 \times 10^{-6}$ s, $e_{\text{ma}} = 0.01$, $p_d = 10^{-8}$, $\lambda_{\text{BSM}} = 0.97$, $F_{\text{init}} = 1.0$, $T_{\text{dp}} = 1.0$ s, $n_{\text{mem}} = 1$, $t_{\text{cut}} = \infty$ s, and $f = 1.16$.

TABLE I. The currently available parameters of multiple experimental platforms according to Ref. [21].

	NV	SiV	Qdot	Ca or Yb	Rb
P_{link}	0.05	0.05	0.1	0.25	0.5
T_P (μs)	1/50	1/30	1/1000	1/0.47	1/5
e_{ma}	0	0	0	0	0
p_d	0	0	0	0	0
λ_{BSM}	1.0	1.0	1.0	1.0	1.0
F_{init}	1.0	1.0	1.0	1.0	1.0
T_{dp} (ms)	10	1	0.003	20	100
n_{mem}	1	1	1	1	1
t_{cut}	$25 \times L/C$	$10 \times L/C$	$0 \times L/C$	$20 \times L/C$	$100 \times L/C$
f	1.0	1.0	1.0	1.0	1.0

TABLE II. The parameters that are potentially achievable in the future for multiple experimental platforms according to Ref. [21].

	NV	SiV	Qdot	Ca or Yb	Rb
P_{link}	0.5	0.5	0.6	0.5	0.7
T_P (μs)	1/250	1/500	1/1000	1/10	1/10
e_{ma}	0	0	0	0	0
p_d	0	0	0	0	0
λ_{BSM}	1.0	1.0	1.0	1.0	1.0
F_{init}	1.0	1.0	1.0	1.0	1.0
T_{dp} (ms)	10000	100	0.3	300	1000
n_{mem}	1	1	1	1	1
t_{cut}	$500 \times L/C$	$50 \times L/C$	$0 \times L/C$	$200 \times L/C$	$500 \times L/C$
f	1.0	1.0	1.0	1.0	1.0

2. Two repeater links for multiple experimental platforms

Reference [21] contains parameters of multiple experimental platforms from research groups in Germany and summarizes them in a model using only P_{link} , T_{dp} and the clock rate f_{clock} . The scenario that we recreate here is referred to as the *node-sends-photons* protocol in Ref. [21], which is a protocol with two repeater links, with entangled pair sources located at the central repeater station, and which also makes use of cutoff times. The comparison of our simulation results with the analytical formulas is shown in Fig. 13 (cf. also the secret key plots in Ref. [21, Fig. 5]). The full parameter sets used are summarized in Tables I and II.

3. Two repeater links with multiple memories

A protocol that makes use of multiple memories and obtains expressions for achievable key rates depending on the number of memories is analyzed in Ref. [23]. It assumes that there is a separate channel for each quantum memory and that trials to establish entangled pairs can be

attempted simultaneously. However, unlike the scenarios that we discuss in the main text, this is not done for both repeater links at the same time. The protocol works as follows.

First, trials are repeated for one of the repeater links until at least one attempt is successful. It is possible that multiple pairs are established in the same trial. Then, trials are performed for the other repeater link until at least one attempt is successful. The quantum memories now containing qubits from successful attempts are paired and entanglement swapping is performed. Finally, if one of the repeater links had more successes than the other, the leftover qubits are discarded. This last step has an effect similar to that of introducing a cutoff-time mechanism, as it prevents qubits from being stored in quantum memories for too long.

We present the key rates calculated from our simulation compared to the analytical expressions in Fig. 14 (see also Ref. [23, Fig. 2]). The parameters for this scenario are as follows: $P_{\text{link}} = 0.0115$, $T_P = 2 \times 10^{-6}$ s, $e_{\text{ma}} = 0.01$, $p_d = 1.8 \times 10^{-11}$, $\lambda_{\text{BSM}} = 0.98$, $F_{\text{init}} = 1.0$, $T_{\text{dp}} = 2.0$ s, $t_{\text{cut}} =$ alternative mechanism, and $f = 1.16$.

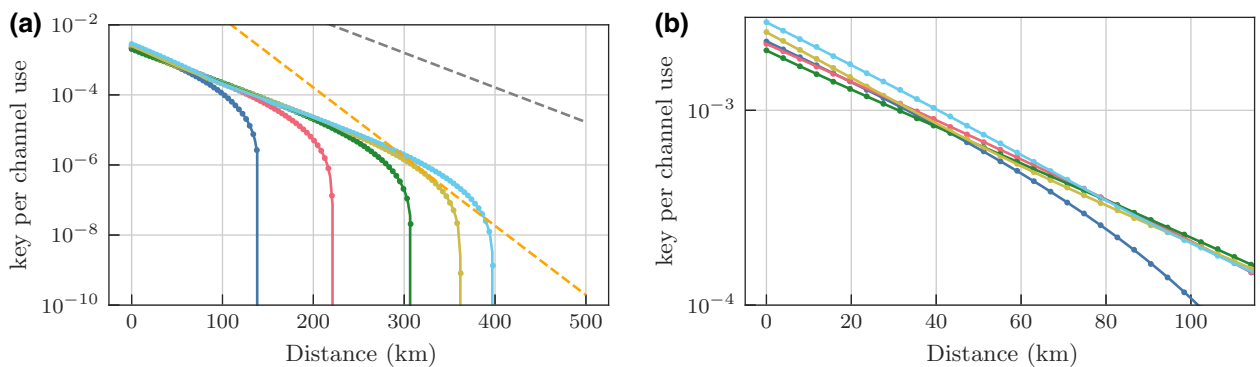


FIG. 14. The obtainable key rates for the multimemory protocol with two repeater links in Ref. [23]. A comparison of the analytical formulas (lines) and our simulation (dots). Results for using one (dark blue), ten (red), 100 (green), 400 (yellow), or 1000 (light blue) memories per repeater link. The orange dashed line is the repeaterless PLOB bound and the gray dashed line is the upper bound for the one-repeater rate [61].

- [1] A. Acin, I. Bloch, H. Buhrman, T. Calarco, C. Eichler, J. Eisert, J. Esteve, N. Gisin, S. J. Glaser, F. Jelezko, S. Kuhr, M. Lewenstein, M. F. Riedel, P. O. Schmidt, R. Thew, A. Wallraff, I. Walmsley, and F. K. Wilhelm, The quantum technologies roadmap: A European Community view, *New J. Phys.* **20**, 080201 (2018).
- [2] N. Gisin, G. Ribordy, W. Tittel, and H. Zbinden, Quantum cryptography, *Rev. Mod. Phys.* **74**, 145 (2002).
- [3] S. Pirandola, U. L. Andersen, L. Banchi, M. Berta, D. Bunandar, R. Colbeck, D. Englund, T. Gehring, C. Lupo, C. Ottaviani, J. Pereira, M. Razavi, J. S. Shaari, M. Tomamichel, V. C. Usenko, G. Vallone, P. Villoresi, and P. Wallden, Advances in quantum cryptography, *Adv. Opt. Photon.* **12**, 1012 (2020).
- [4] M. Hillery, V. Bužek, and A. Berthiaume, Quantum secret sharing, *Phys. Rev. A* **59**, 1829 (1999).
- [5] G. Murta, F. Grasselli, H. Kampermann, and D. Bruss, Quantum Conference Key Agreement: A review, *Adv. Quant. Tech.* **14**, 2000025 (2020).
- [6] J. F. Fitzsimons and E. Kashefi, Unconditionally verifiable blind quantum computation, *Phys. Rev. A* **96**, 012303 (2017).
- [7] H.-J. Briegel, W. Dür, J. I. Cirac, and P. Zoller, Quantum repeaters: The role of imperfect local operations in quantum communication, *Phys. Rev. Lett.* **81**, 5932 (1998).
- [8] W. Dür, H.-J. Briegel, J. I. Cirac, and P. Zoller, Quantum repeaters based on entanglement purification, *Phys. Rev. A* **59**, 169 (1999).
- [9] D. Luong, L. Jiang, J. Kim, and N. Lütkenhaus, Overcoming lossy channel bounds using a single quantum repeater node, *Appl. Phys. B* **122**, 96 (2016).
- [10] L.-M. Duan, M. Lukin, J. I. Cirac, and P. Zoller, Long-distance quantum communication with atomic ensembles and linear optics, *Nature* **414**, 413 (2001).
- [11] A. Boaron, G. Boso, D. Rusca, C. Vulliez, C. Autebert, M. Caloz, M. Perrenoud, G. Gras, F. Bussièrès, M.-J. Li, D. Nolan, A. Martin, and H. Zbinden, Secure quantum key distribution over 421 km of optical fiber, *Phys. Rev. Lett.* **121**, 190502 (2018).
- [12] H.-L. Yin, T.-Y. Chen, Z.-W. Yu, H. Liu, L.-X. You, Y.-H. Zhou, S.-J. Chen, Y. Mao, M.-Q. Huang, W.-J. Zhang, H. Chen, M. J. Li, D. Nolan, F. Zhou, X. Jiang, Z. Wang, Q. Zhang, X.-B. Wang, and J.-W. Pan, Measurement-device-independent quantum key distribution over a 404 km optical fiber, *Phys. Rev. Lett.* **117**, 190501 (2016).
- [13] Y.-A. Chen *et al.*, An integrated space-to-ground quantum communication network over 4,600 kilometres, *Nature* **589**, 214 (2021).
- [14] S. Pirandola, R. Laurenza, C. Ottaviani, and L. Banchi, Fundamental limits of repeaterless quantum communications, *Nat. Commun.* **8**, 15043 (2017).
- [15] M. M. Wilde, M. Tomamichel, and M. Berta, Converse bounds for private communication over quantum channels, *IEEE Trans. Inf. Theory* **63**, 1792 (2017).
- [16] M. Christandl and A. Müller-Hermes, Relative entropy bounds on quantum, private and repeater capacities, *Commun. Math. Phys.* **353**, 821 (2017).
- [17] R. Laurenza, N. Walk, J. Eisert, and S. Pirandola, Rate limits in quantum networks with lossy repeaters, *Phys. Rev. Res.* **4**, 023158 (2022).
- [18] C. Harney and S. Pirandola, End-to-end capacities of imperfect-repeater quantum networks, *Quantum Sci. Technol.* **7**, 045009 (2022).
- [19] S. Muralidharan, L. Li, J. Kim, N. Lütkenhaus, M. D. Lukin, and L. Jiang, Optimal architectures for long distance quantum communication, *Sci. Rep.* **6**, 20463 (2016).
- [20] C. Harney and S. Pirandola, Analytical methods for high-rate global quantum networks, *PRX Quantum* **3**, 010349 (2022).
- [21] P. van Loock, W. Alt, C. Becher, O. Benson, H. Boche, C. Deppe, J. Eschner, S. Höfling, D. Meschede, P. Michler, F. Schmidt, and H. Weinfurter, Extending quantum links: Modules for fiber- and memory-based quantum repeaters, *Adv. Quantum Tech.* **3**, 1900141 (2020).
- [22] E. Shchukin, F. Schmidt, and P. van Loock, Waiting time in quantum repeaters with probabilistic entanglement swapping, *Phys. Rev. A* **100**, 032322 (2019).
- [23] R. Trényi and N. Lütkenhaus, Beating direct transmission bounds for quantum key distribution with a multiple quantum memory station, *Phys. Rev. A* **101**, 012325 (2020).
- [24] L. Kamin, E. Shchukin, F. Schmidt, and P. van Loock, Exact rate analysis for quantum repeaters with imperfect memories and entanglement swapping as soon as possible, *Phys. Rev. Res.* **5**, 023086 (2023).
- [25] T. Coopmans, R. Knegjens, A. Dahlberg, D. Maier, L. Nijsten, J. de Oliveira Filho, M. Papendrecht, J. Rabbie, F. Rozpędek, M. Skrzypczyk, L. Wubben, W. de Jong, D. Podareanu, A. Torres-Knoop, D. Elkouss, and S. Wehner, NetSquid, a NETWORK Simulator for QUANTUM Information using Discrete events, *Commun. Phys.* **4**, 164 (2021).
- [26] R. Satoh, M. Hajdušek, N. Benchasattabuse, S. Nagayama, K. Teramoto, T. Matsuo, S. A. Metwalli, P. Pathumsoot, T. Satoh, S. Suzuki, and R. V. Meter, in *2022 IEEE International Conference on Quantum Computing and Engineering (QCE)* (IEEE, Broomfield, CO, USA, 2022), p. 353.
- [27] X. Wu, A. Kolar, J. Chung, D. Jin, T. Zhong, R. Kettimuthu, and M. Suchara, SeQUeNCe: A customizable discrete-event simulator of quantum networks, *Quantum Sci. Tech.* **6**, 045027 (2021).
- [28] G. Avis, F. Ferreira da Silva, T. Coopmans, A. Dahlberg, H. Jirovská, D. Maier, J. Rabbie, A. Torres-Knoop, and S. Wehner, Requirements for a processing-node quantum repeater on a real-world fiber grid, *npj Quantum Inf.* **9**, 100 (2023).
- [29] F. F. da Silva, A. Torres-Knoop, T. Coopmans, D. Maier, and S. Wehner, Optimizing entanglement generation and distribution using genetic algorithms, *Quantum Sci. Tech.* **6**, 035007 (2021).
- [30] J. Wallnöfer, ReQuSim (2022), <https://doi.org/10.5281/zenodo.7290708>.
- [31] E. Shchukin and P. van Loock, Optimal entanglement swapping in quantum repeaters, *Phys. Rev. Lett.* **128**, 150502 (2022).
- [32] M. Zwerger, H. J. Briegel, and W. Dür, Measurement-based quantum communication, *Appl. Phys. B* **122**, 50 (2016).
- [33] J. Wallnöfer, A. Pirker, M. Zwerger, and W. Dür, Multipartite state generation in quantum networks with optimal scaling, *Sci. Rep.* **9**, 314 (2019).
- [34] O. A. Collins, S. D. Jenkins, A. Kuzmich, and T. A. B. Kennedy, Multiplexed memory-insensitive quantum repeaters, *Phys. Rev. Lett.* **98**, 060502 (2007).

- [35] N. K. Bernardes, L. Praxmeyer, and P. van Loock, Rate analysis for a hybrid quantum repeater, *Phys. Rev. A* **83**, 012323 (2011).
- [36] D. Deutsch, A. Ekert, R. Jozsa, C. Macchiavello, S. Popescu, and A. Sanpera, Quantum privacy amplification and the security of quantum cryptography over noisy channels, *Phys. Rev. Lett.* **77**, 2818 (1996).
- [37] W. Dür and H.-J. Briegel, Entanglement purification for quantum computation, *Phys. Rev. Lett.* **90**, 067901 (2003).
- [38] F. Rozpędek, K. Goodenough, J. Ribeiro, N. Kalb, V. C. Vivoli, A. Reiserer, R. Hanson, S. Wehner, and D. Elkouss, Parameter regimes for a single sequential quantum repeater, *Quantum Sci. Technol.* **3**, 034002 (2018).
- [39] S. Khatri, Policies for elementary links in a quantum network, *Quantum* **5**, 537 (2021).
- [40] S. Khatri, On the design and analysis of near-term quantum network protocols using Markov decision processes, *AVS Quantum Sci.* **4**, 030501 (2022).
- [41] M. Lucamarini, Z. L. Yuan, J. F. Dynes, and A. J. Shields, Overcoming the rate–distance limit of quantum key distribution without quantum repeaters, *Nature* **557**, 400 (2018).
- [42] Á. G. Iñesta, G. Vardoyan, L. Scavuzzo, and S. Wehner, Optimal entanglement distribution policies in homogeneous repeater chains with cutoffs, *npj Quantum Inf.* **9**, 46 (2023).
- [43] M. Gündoğan, J. S. Sidhu, V. Henderson, L. Mazzarella, J. Wolters, D. K. L. Oi, and M. Krutzik, Proposal for spaceborne quantum memories for global quantum networking, *npj Quantum Inf.* **7**, 128 (2021).
- [44] J. Wallnöfer, A. A. Melnikov, W. Dür, and H. J. Briegel, Machine learning for long-distance quantum communication, *PRX Quantum* **1**, 010301 (2020).
- [45] A. Dahlberg and S. Wehner, SimulaQron—a simulator for developing quantum Internet software, *Quantum Sci. Technol.* **4**, 015001 (2018).
- [46] A. Dahlberg, B. van der Vecht, C. D. Donne, M. Skrzypczyk, I. te Raa, W. Kozłowski, and S. Wehner, NetQASM—a low-level instruction set architecture for hybrid quantum-classical programs in a quantum internet, *Quantum Sci. Technol.* **7**, 035023 (2022).
- [47] D. Maier, Master’s thesis, Delft University of Technology and Ludwig-Maximilians-Universität Munich, 2020, <http://resolver.tudelft.nl/uuid:04b9f054-2139-4b30-ba67-4b7b4752ce86>.
- [48] A. Labay Mora, Master’s thesis, Delft University of Technology, 2021, <http://resolver.tudelft.nl/uuid:5dd40a56-8c8d-4766-a2fe-0a8c45e1ee3f>.
- [49] A. Zang, A. Kolar, J. Chung, M. Suchara, T. Zhong, and R. Kettimuthu, in *2022 IEEE International Conference on Quantum Computing and Engineering (QCE)* (IEEE, Broomfield, CO, USA, 2022), p. 617.
- [50] X. Wu, A. Kolar, J. Chung, D. Jin, R. Kettimuthu, and M. Suchara, Parallel simulation of quantum networks with distributed quantum state management (2021), [arXiv:2111.03918](https://arxiv.org/abs/2111.03918) [quant-ph].
- [51] <https://doi.org/10.5281/zenodo.7399897>.
- [52] L. Bennett, B. Melchers, and B. Proppe, Curta: A general-purpose high-performance computer at ZEDAT, Freie Universität Berlin (2020), <https://doi.org/10.17169/refubium-26754>.
- [53] W. Dür and H. J. Briegel, Entanglement purification and quantum error correction, *Rep. Prog. Phys.* **70**, 1381 (2007).
- [54] H.-K. Lo, H. F. Chau, and M. Ardehali, Efficient quantum key distribution scheme and a proof of its unconditional security, *J. Crypt.* **18**, 133 (2005).
- [55] V. Scarani, H. Bechmann-Pasquinucci, N. J. Cerf, M. Dušek, N. Lütkenhaus, and M. Peev, The security of practical quantum key distribution, *Rev. Mod. Phys.* **81**, 1301 (2009).
- [56] M. Tomamichel, C. C. W. Lim, N. Gisin, and R. Renner, Tight finite-key analysis for quantum cryptography, *Nat. Commun.* **3**, 634 (2012).
- [57] D. Bacco, M. Canale, N. Laurenti, G. Vallone, and P. Villoresi, Experimental quantum key distribution with finite-key security analysis for noisy channels, *Nat. Commun.* **4**, 2363 (2013).
- [58] C. C.-W. Lim, F. Xu, J.-W. Pan, and A. Ekert, Security analysis of quantum key distribution with small block length and its application to quantum space communications, *Phys. Rev. Lett.* **126**, 100501 (2021).
- [59] C. H. Bennett, Quantum cryptography using any two nonorthogonal states, *Phys. Rev. Lett.* **68**, 3121 (1992).
- [60] J. Wallnöfer, F. Hahn, M. Gündoğan, J. S. Sidhu, F. Wiesner, N. Walk, J. Eisert, and J. Wolters, Simulating quantum repeater strategies for multiple satellites, *Commun. Phys.* **5**, 169 (2022).
- [61] S. Pirandola, End-to-end capacities of a quantum communication network, *Commun. Phys.* **2**, 51 (2019).